

Temperature enhancement of terahertz responsivity of plasma field effect transistors

Oleg A. Klimenko, Wojciech Knap, Benjamin Iniguez, Dominique Coquillat, Yury A. Mityagin et al.

Citation: *J. Appl. Phys.* **112**, 014506 (2012); doi: 10.1063/1.4733465

View online: <http://dx.doi.org/10.1063/1.4733465>

View Table of Contents: <http://jap.aip.org/resource/1/JAPIAU/v112/i1>

Published by the [American Institute of Physics](#).

Related Articles

Oxygen plasma post process to obtain consistent conductance of carbon nanotubes in carbon nanotube field-effect transistors

Appl. Phys. Lett. **101**, 173104 (2012)

Impact of universal mobility law on polycrystalline organic thin-film transistors

J. Appl. Phys. **112**, 084503 (2012)

Influence of the surface morphology on the channel mobility of lateral implanted 4H-SiC(0001) metal-oxide-semiconductor field-effect transistors

J. Appl. Phys. **112**, 084501 (2012)

Photoresponsivity enhancement of pentacene organic phototransistors by introducing C60 buffer layer under source/drain electrodes

Appl. Phys. Lett. **101**, 163301 (2012)

Photoresponsivity enhancement of pentacene organic phototransistors by introducing C60 buffer layer under source/drain electrodes

APL: Org. Electron. Photonics **5**, 232 (2012)

Additional information on *J. Appl. Phys.*

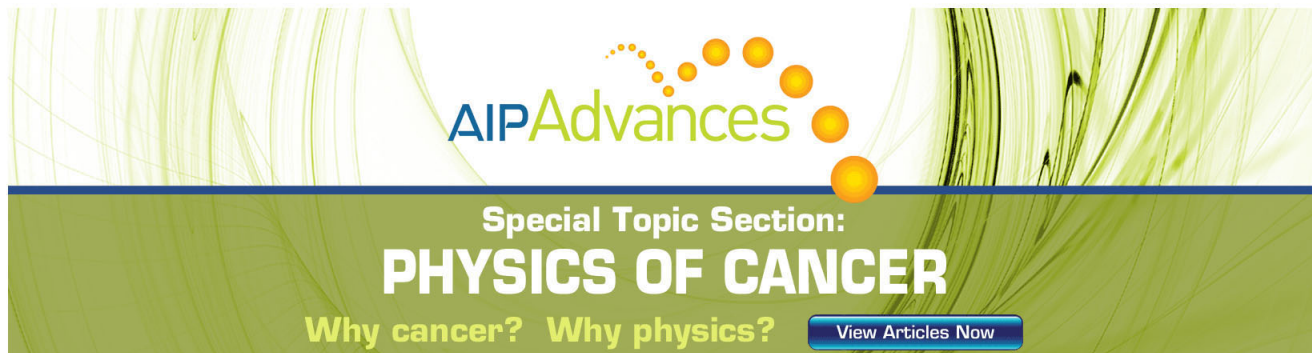
Journal Homepage: <http://jap.aip.org/>

Journal Information: http://jap.aip.org/about/about_the_journal

Top downloads: http://jap.aip.org/features/most_downloaded

Information for Authors: <http://jap.aip.org/authors>

ADVERTISEMENT



AIP Advances

Special Topic Section:
PHYSICS OF CANCER

Why cancer? Why physics? [View Articles Now](#)

Temperature enhancement of terahertz responsivity of plasma field effect transistors

Oleg A. Klimenko,^{1,2} Wojciech Knap,¹ Benjamin Iniguez,³ Dominique Coquillat,¹ Yury A. Mityagin,² Frederic Teppe,¹ Nina Dyakonova,¹ Hadley Videlier,^{1,4} Dmitry But,¹ Francois Lime,³ Jacek Marczewski,⁵ and Krzysztof Kucharski⁵

¹UMR 5221 CNRS, University Montpellier 2, Montpellier 34095, France

²P. N. Lebedev Physical Institute of RAS, Moscow 119991, Russia

³Department of Electronic, Electrical and Automatic Control Engineering, Universitat Rovira i Virgili, Tarragona 43007, Spain

⁴Department of Applied Physics, Tokyo University of Agriculture and Technology, Tokyo 184-8588, Japan

⁵Institute of Electron Technology, Warsaw 02-668, Poland

(Received 19 December 2011; accepted 5 June 2012; published online 5 July 2012)

Temperature dependence of THz detection by field effect transistors was investigated in a wide range of temperatures from 275 K down to 5 K. The important increase of the photoresponse following $1/T$ functional dependence was observed when cooling from room temperature down to 30 K. At the temperatures below ~ 30 K, the THz response saturated and stayed temperature independent. Similar behavior was observed for GaAs, GaN, and Si based field effect transistors. The high temperature data were successfully interpreted using recent theory of overdamped plasma excitation in field effect transistors. The low temperature saturation of the photoresponse was tentatively explained by the change of the transport regime from diffusive to ballistic or traps governed one. Our results clearly show that THz detectors based on field effect transistors may improve their responsivity with lowering temperature but in the lowest temperatures (below ~ 30 K) further improvement is hindered by the physics of the electron transport itself. © 2012 American Institute of Physics. [<http://dx.doi.org/10.1063/1.4733465>]

I. INTRODUCTION

Field effect transistors (FETs) were recently shown to be efficient THz detectors and emitters.^{1–5} With its high operation speed and well developed microcircuit chips fabrication technology, FETs become the most favorable devices for fast THz detection that is required for THz scanning or THz imaging systems.^{6,7}

The mechanism of THz radiation detection by FETs was first proposed by Dyakonov and Shur.^{1,2} They have shown that the 2D electron gas in FETs can be described by nonlinear hydrodynamic equations. THz radiation may excite plasma density oscillations and plasma waves in the FET channel. Plasma nonlinearities lead to THz rectification. As the result, a constant source-drain voltage appears which is called the photovoltaic response, or the photoresponse. Depending on the parameters, a FET can operate as a resonant or broadband detector. In the resonant case, when the plasma damping is low and transistor channel is short enough, the transistor channel may serve as the resonator cavity for the plasma waves. The eigenfrequency of such resonator can be adjusted by the gate voltage. In the case of long channels or low carrier mobility, the photoresponse weakly depends on the radiation frequency leading to broadband detection.⁶

Both types of THz detection by FETs were discovered and studied experimentally.^{8–14} And the Dyakonov-Shur theory was also developed more in detail.^{15,16} But after these multiple studies, questions about the physical limits of the THz sensitivity and about the best operating temperature remain unclear.

In this paper, we investigate different III-V and Si FETs as broadband THz detectors in a temperature range from 300 K down to 5 K. The important increase of the photoresponse following $1/T$ functional dependence is reported when cooling down to 30 K. At the lowest temperatures below ~ 30 K, the temperature independent behavior (saturation) is observed. The high temperature data are interpreted using a physical model based on a diffusive transport approach. The low temperature saturation of the photoresponse is tentatively explained by a limitation of the diffusive transport approach related to the change of the transport regime from diffusive to ballistic¹⁷ or trap governed one.^{18,19}

II. EXPERIMENTAL DETAILS

Three types of FETs made of different materials by different technologies (GaN HEMT,⁴ GaAs HEMT,¹¹ and Si MOSFET) were studied. For all transistors, we have compared the photoresponse on the gate voltage dependence with its DC transfer characteristics. This comparison was made for different transistor temperatures (from 5 to 275 K). The incident radiation coupling was performed by the bonding wires and contact pads,⁶ and asymmetry of the source drain and source gate capacitances decided about the sign of the detection signal. Independently of the material and device geometry, high temperature results for all investigated were similar and could be interpreted in the frame of the same theoretical model.

Table I shows the main parameters of the transistors, such as the gate length, L_g , and width, W_g , the electron effective mass in the channel, m_{eff} , the electron mobility, μ_0 , and

TABLE I. Main parameters of studied transistors.

Transistor	L_g (μm)	W_g (μm)	m_{eff}/m_e	μ_0 , at 300 K $\text{cm}^2/(\text{V s})$	μ_0 , at 4 K $\text{cm}^2/(\text{V s})$	$\lambda_{300\text{K}}$ (μm) deg./nondeg.	$\lambda_{4\text{K}}$ (μm) deg./nondeg.
GaN HEMT	0.25	100	0.2	1500	20 000	0.03/0.04	0.46/0.07
GaAs HEMT	0.25	200	0.067	6500	30 000	0.09/0.11	0.41/0.06
Si MOSFET	10	5	0.19	500	500	0.001/0.01	0.001/0.002

the mean free path at room temperature, $\lambda_{300\text{K}}$, and at liquid helium temperature, $\lambda_{4\text{K}}$. The mean free path was calculated in two cases: (i) high carrier density degenerate gas corresponding to the open state of transistors, and (ii) low carrier density nondegenerate electron gas corresponding to gate voltages close to the threshold.

We have used a 0.3 THz electronic source for detection measurements. The studied transistor was placed into a liquid helium cooled continuous flow cryostat allowing setting any sample temperature between 5 K and 300 K with ~ 0.1 K precision. The four parabolic mirrors based optical system was used to focus the incident radiation to ~ 4 mm diameter spot. The system enabled also precise adjustment of the spot position, the way to provide maximal asymmetry of the transistor channel excitation (between the source side and the drain side) and hence leading to a maximal photoresponse signal. The incident radiation was modulated by a chopper at frequency 484 Hz, and the photoresponse was measured by a standard lock-in technique¹⁶ using a preamplifier ($\times 25$) with the pass band 300 Hz–1000 kHz, 6 dB/octave, and the input resistance 10 M Ω . The capacitance of cables connecting the transistor to the preamplifier equaled 200 pF, so the cable impedance was 1.6 M Ω .

III. RESULTS

Figures 1(a), 2(a), and 3(a) show DC transfer characteristics ($I_{DS}(V_g)$) of studied GaAs and GaN HEMTs and Si MOSFET for different transistor temperatures. As one can see, the threshold voltage changes, and the slope becomes steeper with decreasing temperature.

The results of photoresponse measurements for GaAs, GaN, and Si FETs at different temperatures are presented in Figures 1(b), 2(b), and 3(b). The maxima of the signal shift towards higher gate voltages with decreasing the temperature following the threshold voltage on DC transfer characteristics. The value of the maximal photoresponse rises with cooling the transistor down, and it saturates for temperatures of 30 K and lower.

We will analyze the results using recently found relation between the photoresponse and the channel conductivity:¹⁶

$$\Delta U = \frac{U_a^2}{4} \left[\frac{1}{\sigma} \frac{d\sigma}{dU} \right]_{U=U_0}, \quad \text{or} \quad (1)$$

$$\Delta U = \frac{U_a^2}{4} \frac{d(\ln \sigma)}{dU} \Big|_{U=U_0} = \frac{U_a^2}{4} \frac{d}{dV_g} \ln I_{DS}(V_g), \quad (2)$$

where ΔU is the photoresponse, σ is the conductivity, $I_{DS}(V_g)$ is DC drain-source current dependence on the gate voltage (the DC transfer characteristics), U_a is the amplitude of the

AC gate-to-source voltage induced by the incident THz radiation (it reflects the antenna coupling efficiency and the power of the THz source), U_0 is averaged by time and the channel length voltage swing $U_0 = V_g - V_{th}$ (V_{th} is the threshold voltage), U is local voltage swing depending on the coordinates and taking into account the AC voltage induced by THz.

For the correct comparison the loading effects caused by the finite impedance of the read-out circuit, Z_L , have to be taken into account.¹⁶ The impedance Z_L can be written as

$$\frac{1}{Z_L} = \frac{1}{R_{IN}} + i\omega C, \quad (3)$$

where R_{IN} is the input resistance of the pre-amplifier, C is the capacitance of the cables between the transistor and the pre-amplifier, and ω is the modulation frequency of the incident THz radiation.

Finally, one can simulate/compare the measured photoresponse with the following function:

$$V_{fit} = A \frac{d}{dV_g} \ln I_{DS}(V_g) \frac{1}{1 + R_{CH}/Z_L}. \quad (4)$$

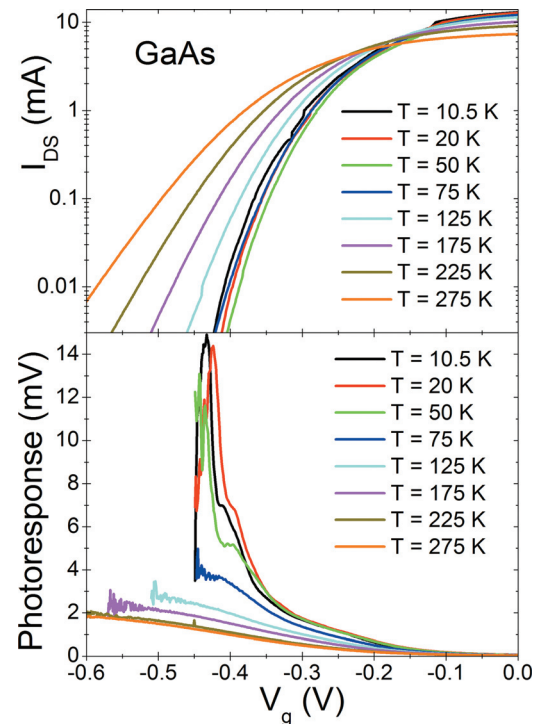


FIG. 1. Measured transfer characteristics (a) and photoresponse on gate voltage dependences (b) of studied GaAs HEMT at different temperatures from 275 K to 10 K. The temperature values are listed on the graph.

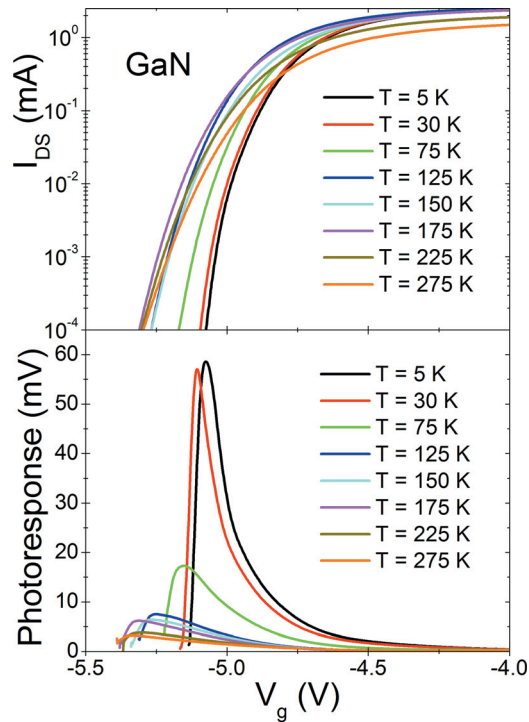


FIG. 2. Measured transfer characteristics (a) and photoresponse on gate voltage dependences (b) of studied GaN HEMT at different temperatures from 275 K to 5 K. The temperature values are listed on the graph.

In what follows, we will call V_{fit} the calculated signal. Here A is the fitting parameter reflecting the antenna efficiency.

Figures 4–6 show the comparison of the measured photoresponse (dots) and the calculated signal V_{fit} (solid line).

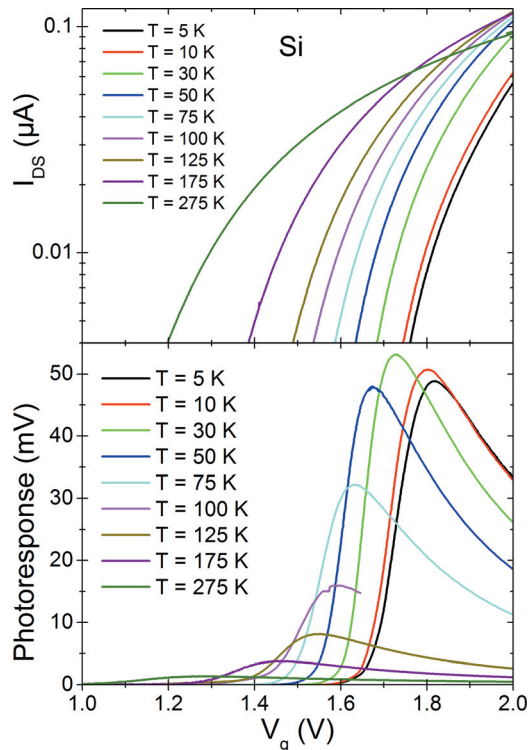


FIG. 3. Measured transfer characteristics (a) and photoresponse on gate voltage dependences (b) of studied Si MOSFET at different temperatures from 275 K to 5 K. The temperature values are listed on the graph.

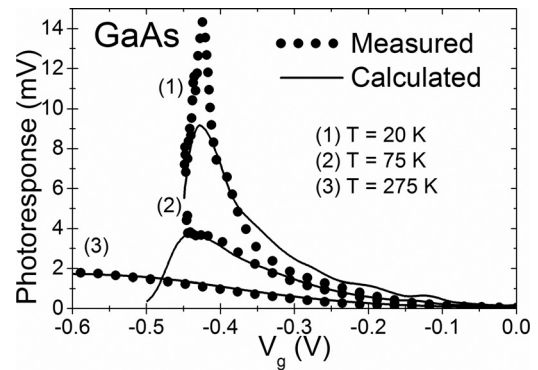


FIG. 4. Comparison of directly measured (dots) and calculated (solid line) from transfer characteristics by Eq. (4) photoresponse on gate voltage dependences of GaAs HEMT for different temperatures (20 K, 75 K, 275 K). For the fitting parameter, we have used following values: $A = 6.5 \times 10^{-5} \text{ V}^2$ at $T = 275 \text{ K}$, $A = 5.3 \times 10^{-5} \text{ V}^2$ at $T = 75 \text{ K}$, $A = 9.5 \times 10^{-5} \text{ V}^2$ at $T = 20 \text{ K}$.

The results for different materials and temperatures are shown. The values of the normalizing factor A are given in the figure captions. The general result is that the calculations can well reproduce the shape of the photoresponse for all studied transistors at all temperatures.

All studied transistors had not specially designed THz antenna, and the incident radiation coupling was performed by the bonding wires⁶ and contact pads with a comparable efficiency. It explains similarity of the factor A values of different transistors that were obtained from fitting.

Summarizing this part, the behavior of the broadband THz photoresponse of all investigated FETs can be well reproduced by calculations using Eq. (1). This means that in the case of the broadband THz detection, the knowledge of the transfer characteristics and loading impedances are sufficient to predict the shape of the photoresponse versus gate voltage curve.

IV. DISCUSSION

Let us discuss closer the relation between the conductivity and maximum responsivity of FETs. In the case of the gate voltage well above the threshold (open transistor), the conductivity depends linearly on the gate voltage,

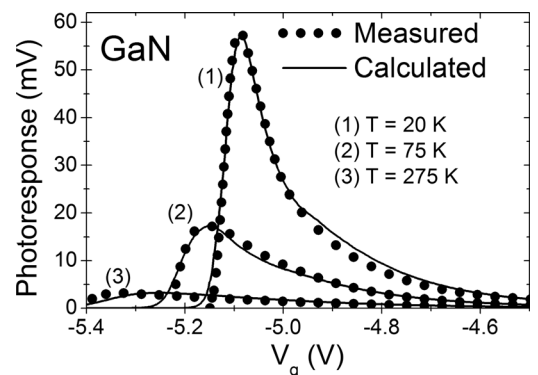


FIG. 5. Comparison of directly measured (dots) and calculated (solid line) from transfer characteristics by Eq. (4) photoresponse on gate voltage dependences of GaN HEMT for different temperatures (20 K, 75 K, 275 K). For the fitting parameter, we have used following values: $A = 1.29 \times 10^{-4} \text{ V}^2$ at $T = 275 \text{ K}$, $A = 3.96 \times 10^{-4} \text{ V}^2$ at $T = 75 \text{ K}$, $A = 9.15 \times 10^{-4} \text{ V}^2$ at $T = 20 \text{ K}$.

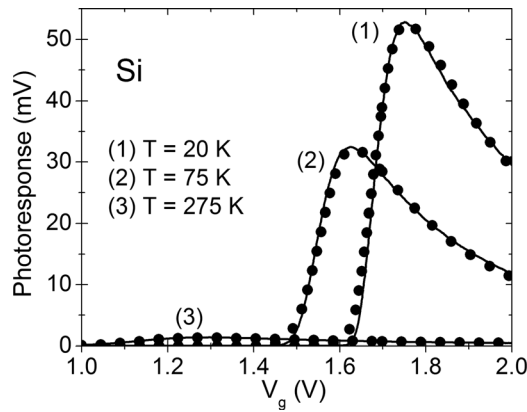


FIG. 6. Comparison of directly measured (dots) and calculated (solid line) from transfer characteristics by Eq. (4) photoresponse on gate voltage dependences of Si MOSFET for different temperatures (20 K, 75 K, 275 K). For the fitting parameter, we have used following values: $A = 3.65 \times 10^{-4} \text{ V}^2$ at $T = 275 \text{ K}$, $A = 3.79 \times 10^{-3} \text{ V}^2$ at $T = 75 \text{ K}$, $A = 6.1 \times 10^{-3} \text{ V}^2$ at $T = 20 \text{ K}$.

$\sigma \propto V_g - V_{th}$, and the calculated by Eq. (1) photoresponse takes the form

$$\Delta U = \frac{U_a^2}{4} \frac{1}{V_g - V_{th}}. \quad (5)$$

This formula was originally obtained by Dyakonov and Shur in Ref. 2. One can see that the signal diverges approaching the threshold voltage. This divergence was never observed, because in the near-threshold and subthreshold regions the linear approximation for the conductivity is not valid anymore. For the subthreshold region (closed transistor), one should use the exponential approximation instead¹⁵

$$\sigma \propto \exp\{(V_g - V_{th})/U^*\}, \quad (6)$$

where U^* is the subthreshold slope. In this case, the photoresponse is saturated, and its maximum value obtained from Eq. (1) is given by

$$\Delta U \text{ max} = \frac{U_a^2}{4U^*}. \quad (7)$$

Eq. (7) shows that the maximal value of the photoresponse depends only on the subthreshold slope U^* . In the case when the current is due to the diffusion or thermionic emission mechanisms, the subthreshold slope is proportional to the temperature¹⁵

$$U^* = \eta kT/e, \quad (8)$$

where η is the ideality factor. According to Eqs. (7) and (8), one can expect that with decreasing temperature the subthreshold slope U^* will decrease and consequently the maximum responsivity will increase linearly.

By analyzing the experimental transfer characteristics, we determined the temperature dependence of the subthreshold slope U^* for all investigated transistors. Results are shown in Fig. 7. One can see that approximation of linearity of the subthreshold U^* as given by Eq. (8) is valid only down to temperatures of around 30 K. At lower temperatures ($T < 30 \text{ K}$) U^* saturates, for all investigated FETs.

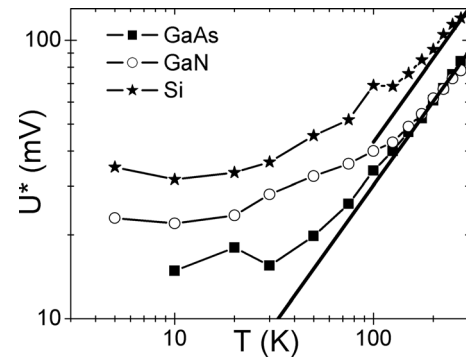


FIG. 7. Temperature dependence of the subthreshold slope, U^* , obtained from transfer characteristics measurements for all studied transistors. Squares are GaAs HEMT, circles are GaN HEMT, stars are Si MOSFET, solid lines represent Eq. (8) for different values of η . Linear dependence at high temperatures ($T > 150 \text{ K}$) is defined by diffusive current; the saturation at low temperatures ($T < 30 \text{ K}$) can be caused by the effect of an increasing interface state density.

This explains similar saturation with lowering temperature observed in the photoresponse maxima, $\Delta U \text{ max}$, shown in Fig. 8. Being inversely proportional to U^* , photoresponse increases with decreasing the temperature, and then it saturates for all transistors.

The observed nonlinearity and saturation in U^* and $\Delta U \text{ max}$ temperature dependences can be explained by the change of the dominating transport mechanism. When the temperature is high enough, the diffusion current dominates. With lowering the temperature, contribution of one of supplementary current mechanisms such as ballistic current or trap governed one can become dominant. It results in deviation of temperature dependence of U^* from the linear one. The temperature dependence of $\Delta U \text{ max}$ becomes nonlinear as well.

In the case of the ballistic current, a mean free path for electrons, λ , should exceed the gate length. For all studied transistors the mean free path was calculated in two cases: (i) high carrier density degenerate gas corresponding to the open state of the transistors and (ii) low carrier density non-degenerate electron gas corresponding to gate voltages close to the threshold (see Table I). In the first case, the electron velocity is given by the Fermi velocity, whereas in the second one it is given by the thermal velocity. One can see that

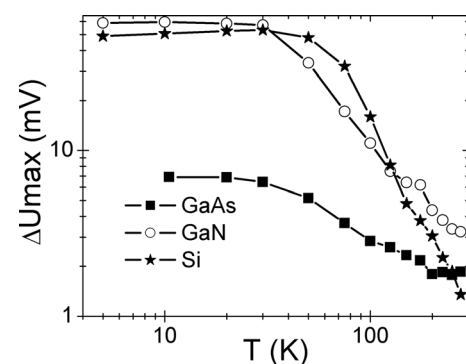


FIG. 8. Evaluation of the maximal photoresponse value with the temperature for all studied transistors. Squares are GaAs HEMT, circles are GaN HEMT, and stars are Si MOSFET.

at cryogenic temperatures the mean free path of electrons in the open channel is comparable with the gate length for GaAs and GaN based transistors. Therefore, the low temperature operation in the open state (far from threshold) of these FETs can be explained by ballistic transport,^{17,20,21} in which the drain-to-source current becomes temperature independent. However, close to the threshold and in the sub-threshold range, when the photoresponse is maximal, the mean free path is always shorter than the gate length for all transistors. Therefore, the saturation of the photoresponse in this region should be attributed to another mechanism like the traps or impurity band related transport.

At room temperature, kinetic energy of electrons ($kT \sim 25$ meV) is relatively high and some traps with low binding energy are inactive. With lowering temperature, these traps can bind electrons. The density of electrons trapped in the interface states is not affected by the gate voltage. Therefore, an increase of the number of electrons trapped by interface states may result in the deviation from the linear dependence of the subthreshold slope on temperature, which is valid in the diffusion regime (higher temperatures)—described by Eq. (8). Further studies are clearly needed to answer the question which of these mechanisms (ballistic or trap governed one) dominates and is responsible for the temperature saturation of the THz photoresponse in FETs. A combination of both mechanisms can also take place. Currently, we can only suppose that the ballistic regime most likely dominates in the case of GaAs and GaN HEMTs in the open channel state. Whereas the maximum photoresponse in all investigated FETs takes place in the subthreshold range and its saturation with temperature is probably caused by nondiffusive transport related to the traps or impurity bands forming the tails of the density states close to conduction band.

V. CONCLUSION

We have studied broadband THz photoresponse of different GaInAs/GaAs, GaN/AlGaIn, and Si FETs in temperature range 5–275 K. We have analyzed the results using a recent theoretical model and shown that the shape of the photoresponse on the gate voltage dependence is defined by the transfer characteristics at all temperatures down to 5 K. The photoresponse increased by about one order of magnitude with decreasing of the transistor temperature down to 30 K. For lower temperatures, the photoresponse value was saturated, probably due to the change of the dominant electron transport mechanism. Our results clearly show that THz detectors based on GaAs, GaN, or Si field effect transistors can be improved by lowering temperature down to ~ 30 K. They show also however that below 30 K the further

improvement is hindered by the physics of the detection process itself.

ACKNOWLEDGMENTS

We thank Professor S. Bollaert and Dr. Y. Rollens (IEMN-UMR 5820) for providing GaN HEMTs. This work was supported by the JST-ANR WITH project, the European Union under Contracts Nos. 218255 and 216171, the International GDR project, the French embassy in Moscow, the CNRS, and the Catalan Government under project 2010 CONE2 00061.

- ¹M. I. Dyakonov and M. S. Shur, *Phys. Rev. Lett.* **71**, 2465 (1993).
- ²M. I. Dyakonov and M. S. Shur, *IEEE Trans. Electron Devices* **43**, 380 (1996).
- ³W. Knap, J. Łusakowski, T. Parenty, S. Bollaert, A. Cappy, V. V. Popov, and M. S. Shur, *Appl. Phys. Lett.* **84**, 3523 (2004).
- ⁴A. El Fatimy, N. Dyakonova, Y. Meziani, T. Otsuji, W. Knap, S. Vandembrouk, K. Madjour, D. Théron, C. Gaquiere, M. A. Poisson, S. Delage, P. Pristawko, and C. Skierbiszewski, *J. Appl. Phys.* **107**, 024504 (2010).
- ⁵N. Dyakonova, A. El Fatimy, J. Łusakowski, W. Knap, M. I. Dyakonov, M. A. Poisson, E. Morvan, S. Bollaert, A. Shchepetov, Y. Roelens, Ch. Gaquiere, D. Theron, and A. Cappy, *Appl. Phys. Lett.* **88**, 141906 (2006).
- ⁶W. Knap, M. Dyakonov, D. Coquillat, F. Teppe, N. Dyakonova, J. Łusakowski, K. Karpierz, G. Valusis, D. Seliuta, I. Kasalynas, A. El Fatimy, and T. Otsuji, *J. Infrared Millim. Terahz. Waves* **30**, 1319 (2009).
- ⁷W. Knap, F. Teppe, N. Dyakonova, D. Coquillat, and J. Łusakowski, *J. Phys.: Condens. Matter* **20**, 384205 (2008).
- ⁸W. Knap, Y. Deng, S. Romyantsev, and M. S. Shur, *Appl. Phys. Lett.* **81**, 4637 (2002).
- ⁹W. Knap, Y. Deng, S. Romyantsev, J.-Q. Lu, M. S. Shur, C. A. Saylor, and L. C. Brunel, *Appl. Phys. Lett.* **80**, 3433 (2002).
- ¹⁰A. El Fatimy, F. Teppe, N. Dyakonova, W. Knap, D. Seliuta, G. Valušis, A. Shchepetov, Y. Roelens, S. Bollaert, A. Cappy, and S. Romyantsev, *Appl. Phys. Lett.* **89**, 131926 (2006).
- ¹¹S. Nadar, H. Videllier, D. Coquillat, F. Teppe, M. Sakowicz, N. Dyakonova, W. Knap, D. Seliuta, I. Kašalynas, and G. Valušis, *J. Appl. Phys.* **108**, 054508 (2010).
- ¹²W. Knap, F. Meziani, N. Dyakonova, J. Łusakowski, F. Boeuf, T. Skotnicki, D. Maude, S. Romyantsev, and M. S. Shur, *Appl. Phys. Lett.* **85**, 675 (2004).
- ¹³R. Tauk, F. Teppe, S. Boubanga, D. Coquillat, W. Knap, Y. Meziani, C. Gallon, F. Boeuf, T. Skotnicki, C. Fenouillet-Beranger, D. K. Maude, S. Romyantsev, and M. S. Shur, *Appl. Phys. Lett.* **89**, 253511 (2006).
- ¹⁴F. Schuster, D. Coquillat, H. Videllier, M. Sakowicz, F. Teppe, L. Dussopt, B. Giffard, T. Skotnicki, and W. Knap, *Opt. Express* **19**, 7827 (2011).
- ¹⁵W. Knap, V. Kachorovskii, Y. Deng, S. Romyantsev, J.-Q. Lu, R. Gaska, M. S. Shur, G. Simin, X. Hu, M. Asif Khan, C. A. Saylor, and L. C. Brunel, *J. Appl. Phys.* **91**, 9346 (2002).
- ¹⁶M. Sakowicz, M. B. Lifshits, O. A. Klimenko, F. Schuster, D. Coquillat, F. Teppe, and W. Knap *J. Appl. Phys.* **110**, 054512 (2011).
- ¹⁷M. Staedele, in Proceedings of ESSDERC (2002).
- ¹⁸J. A. Martino, E. Simoen, and C. Claeys, *Solid-State Electron.* **38**, 1799 (1995).
- ¹⁹W. C. Kao, M.Sc. Thesis, Pennsylvania State University, 2010.
- ²⁰H. Kawaura, *Silicon Nanoelectronics* (CRC, 2005), pp. 65–87.
- ²¹D. Jiménez, J. J. Sáenz, B. Iñiguez, J. Suñé, L. F. Marsal, and J. Pallarès, *J. Appl. Phys.* **94**, 1061 (2003).